



**EUROfusion**

WPMAT-CPR(17) 17062

A Galatanu et al.

## **Thermal barriers for DEMO W-monoblock divertor**

Preprint of Paper to be submitted for publication in Proceeding of  
16th International Conference on Plasma-Facing Materials and  
Components for Fusion Applications



This work has been carried out within the framework of the EUROfusion Consortium and has received funding from the Euratom research and training programme 2014-2018 under grant agreement No 633053. The views and opinions expressed herein do not necessarily reflect those of the European Commission.

This document is intended for publication in the open literature. It is made available on the clear understanding that it may not be further circulated and extracts or references may not be published prior to publication of the original when applicable, or without the consent of the Publications Officer, EUROfusion Programme Management Unit, Culham Science Centre, Abingdon, Oxon, OX14 3DB, UK or e-mail [Publications.Officer@euro-fusion.org](mailto:Publications.Officer@euro-fusion.org)

Enquiries about Copyright and reproduction should be addressed to the Publications Officer, EUROfusion Programme Management Unit, Culham Science Centre, Abingdon, Oxon, OX14 3DB, UK or e-mail [Publications.Officer@euro-fusion.org](mailto:Publications.Officer@euro-fusion.org)

The contents of this preprint and all other EUROfusion Preprints, Reports and Conference Papers are available to view online free at <http://www.euro-fusionscipub.org>. This site has full search facilities and e-mail alert options. In the JET specific papers the diagrams contained within the PDFs on this site are hyperlinked

# Thermal barriers for DEMO W-monoblock divertor

Magdalena Galatanu<sup>1,2</sup>, Monica Enculescu<sup>1</sup>, Andrei Galatanu<sup>1</sup>

<sup>1</sup>*National Institute of Materials Physics, Atomistilor Street 405 A, Magurele, Ilfov 077125, Romania*

<sup>2</sup>*Doctoral School in Physics, University of Bucharest, Atomistilor Street 405, Magurele, Ilfov 077125, Romania*

DEMO fusion reactor divertor is expected to extract a heat flux of about 10 MW/m<sup>2</sup>. One of the most promising concept design for it is the W-monoblock, which should be connected to a CuCrZr or an advanced Cu ODS alloy pipe passing through the W component. Since the optimum operating temperature windows for W and existing Cu alloys are far away from overlapping, a suited interface is needed to keep the cooling pipe temperature below 350-400 °C while the W part might be heated up to 800 °C or more at the joint level. The interface material should therefore have a low enough thermal conductivity to protect the pipe from overheating and the W-pipe joint from stresses induced by the different thermo-mechanical properties of W and Cu-alloys. As interface materials we have considered Cu-ZrO<sub>2</sub> composites produced by powder metallurgy route. Such materials can be realized in an unexpected large compositional range (up to at least 90% ZrO<sub>2</sub> volume concentration) and be easily further joined to both W and Cu-alloys by an electrical field assisted technology. We analyse their microstructure and thermo-physical properties both as single materials and included in W-thermal barrier-CuCrZr 3-layers systems in comparison to those of previously produced Cu based composites and commercially available Cu foams.

PACS:

65.40.-b Thermal properties of crystalline solids

81.05.Zx New materials: theory, design, and fabrication

72.15.Eb Electrical and thermal conduction in crystalline metals and alloys

Keywords: thermal barriers, powder metallurgy, spark plasma sintering, thermo-physical properties

## 1. Introduction

DEMO is a key point in the European fusion roadmap, being a fusion reactor able to produce energy to the grid. The materials used for it should withstand both high heat fluxes and intense neutron irradiation for long times, ranging between 2 and 5 years [1]. In the case of its divertor, an expected heat flux of about 10-20 MW/m<sup>2</sup> should be extracted. Thus, a full W armour is considered as the most viable option, while the following heat sink part will be most likely constructed from Cu or ODS Cu alloys pipes [2], similar to the ITER full-W divertor design [3]. W has a high melting point, a high sputtering threshold and low tritium retention [4,5], which are desired properties for a plasma facing material, but W also has a rather high ductile-brittle transition temperature (DBTT), around 300°C. This value sets the lower limit of its operating temperature window, while the upper limit can be derived from recrystallization constraints at about 1200 °C. In fact, the optimum operating temperature for W is considered to be around 800-1000 °C, taking into account recovery considerations [6-9]. To remove the large heat flux from the divertor, materials with high thermal conductivity are needed in the heatsink. Such materials will support the W components and will be also exposed to neutron irradiation. Thus high strength and good irradiation behaviour are also required properties. One already characterized candidate is the Cu precipitate strengthened (PS) alloy CuCrZr [10] or similar oxide dispersion strengthened (ODS) Cu alloys. For CuCrZr alloys the temperature operating window is between 180°C and about 350°C [11, 12]. The upper limit value is considerably lower as the W optimal operation temperature. To keep both materials in their respective operating temperature ranges an interface material is needed. Such a material should slow down the heat transfer from the W hot part to the CuCrZr cool part, acting like a thermal

barrier (TB) [13-15]. In the same time, taking into account the large difference between the W and Cu thermal expansion coefficients (CTE), it is important that the interface material will have a CTE value in-between, thus decreasing the thermal generated stresses [16]. To solve this particular problem, different interface materials have been suggested [17-21], but these have also thermal conductivities between Cu and W values and therefore are not acting like a proper thermal barrier. Our previous work [15] has shown that some Cu based composites can be efficient thermal barrier materials, while mitigating in the same time the effects of the different thermal expansion coefficients of W and Cu (CuCrZr). In the W-monoblock divertor concept [12] the W armour is formed as a rectangular prism and a CuCrZr pipe is passing through the W component. In this case the thermal barrier will create a functional joint between the armour and heatsink and should be thinner as 1 mm. These means, taking into account the large temperature difference between W and CuCrZr optimum operating temperatures, very low thermal conductivities values for the interface material, if possible smaller than 10 W/m/K [14]. For these reasons, in the present work, we have considered Cu-ZrO<sub>2</sub> composites as potential candidates for a DEMO divertor thermal barrier material. ZrO<sub>2</sub> is a ceramic material having a high melting temperature, with one of the lowest thermal conductivities for such oxides, and a good compatibility with Cu. For the obtained materials we investigate the sintering behaviour, the resulting morphology and the relevant thermo-physical properties. The possible joining of the thermal barrier with W and CuCrZr is also evaluated.

## 2. Experimental

The Cu-ZrO<sub>2</sub> thermal barrier materials have been prepared using micrometric Cu powders (average particle size, APS = 1  $\mu$ m) and nanometric ZrO<sub>2</sub> powders (APS = 20 nm) provided by US Research Nanomaterials, Inc. The powders have been mixed in Ar protective atmosphere in various volume proportions, ranging from 10 to 90 % for the dispersed materials, using a planetary ball mill at low speed (50 rpm). The homogenized compositions have been sintered in graphite moulds using a spark plasma sintering (SPS) equipment at different temperatures for 5 min. Since the real temperature inside the moulds can be only approximated in the following the SPS average control temperature will be used to discriminate between samples. The maximum sintering temperature which can be used was determined by the limit at which Cu starts to melt. The thermal barriers have been connected to W and CuCrZr using the same SPS equipment.

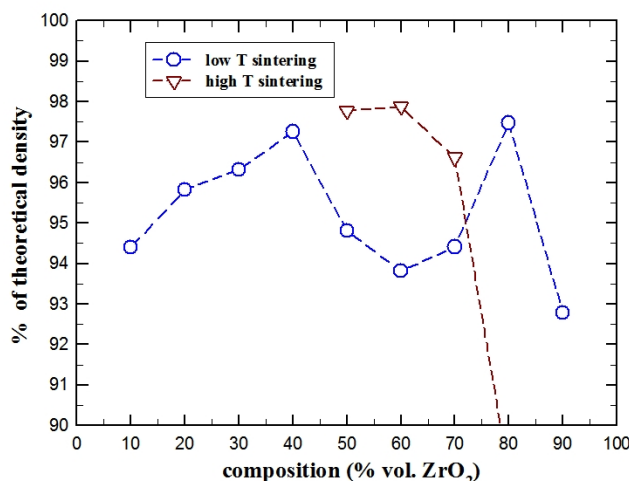
The samples' morphology was checked by SEM using a microscope equipped with backscattering detector (BSD), used to evaluate the distribution of the elements in the sample. The thermal transport properties have been investigated using a Netzsch LFA 457 Microflash up to 1000 °C and the expansion coefficients have been determined in the same temperature range using a Netzsch 402 C dilatometer. The electrical resistivity was measured up to 800 °C using a SBA 458 Netzsch equipment, in a 4 contact point configuration. The LFA equipment allows the direct measurement of the thermal diffusivity, while the specific heat of materials, can be determined by a differential method using a reference sample. The thermal conductivity is calculated by  $\lambda = \alpha \times \rho \times C_p$ , with  $\rho$  the density and  $\alpha$  the diffusivity of the material. In the case of a 2-layer sample, assuming the thermal properties are known for each material layer, the thermal contact resistance can be determined and used to evaluate the joint quality. The samples' density was measured by Archimedes method using a high resolution balance.

## 3. Results and discussion

### 3.1. Sintering of Cu-ZrO<sub>2</sub> specimens

The SPS technology is based on a multitude of effects, resulting in high heating and cooling

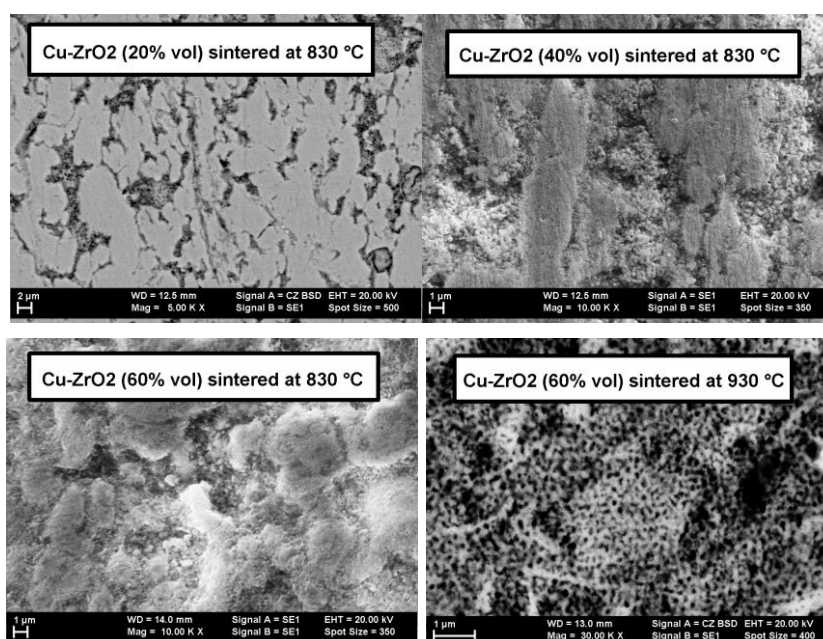
rates and very short overall processing time. This is because the heating arises from high intensity dc current pulses trains applied to the graphite mould and sample at the same time. While the current flowing through the mould provides a convection heating from outside, the current flowing through samples is on one side heating the metallic materials by Joule effect and on the other side creating small electric discharges at the imperfect grains connections [22]. This phenomena is assumed to be responsible for mass transfer and an enhanced sintering. For ceramic samples, the high intensity current flows on the surface of the grains and again is supposed to produce discharges and mass transfer at the imperfect grain connections [23]. In the case of metal-ceramic composites, the phenomenology is more complicated and difficult to quantify. If the volume fraction of metal is high, the current will flow through the metal increasing its temperature. Thus if the melting temperature of the metal is considerably lower than the melting temperature of the ceramic, the metal part will be overheated resulting in a catastrophic melt of the sample. On the other hand, if the ceramic volume fraction is high, one can expect that above a threshold ceramic concentration the sample will be in the best case only partially sintered (e.g. metal-metal connections and eventually metal-ceramic connections). This limitation was expected to occur also in the case of Cu-ZrO<sub>2</sub> composites. To increase the composition range we have chosen to use nanometric oxide powders which should allow a better dispersion in the Cu matrix. As in the case of Cu-Al<sub>2</sub>O<sub>3</sub> or Cu-Y<sub>2</sub>O<sub>3</sub> composites [15], a maximum oxide concentration of about 50% volume was expected. Surprisingly, in the present case, we have been able to consolidate specimens with ZrO<sub>2</sub> volume concentrations up to 90%. Up to a volume concentration of about 80% ZrO<sub>2</sub> a SPS average temperature of 830 °C can be used to obtain well consolidated materials. Higher temperatures can be used at lower ZrO<sub>2</sub> content (like e.g. 930 °C, up to 70%). Increased temperatures result in a small amount of melted Cu emerging from the samples.



**Fig. 1.** Relative densities of Cu-ZrO<sub>2</sub> composites sintered at 830 °C and 930 °C.

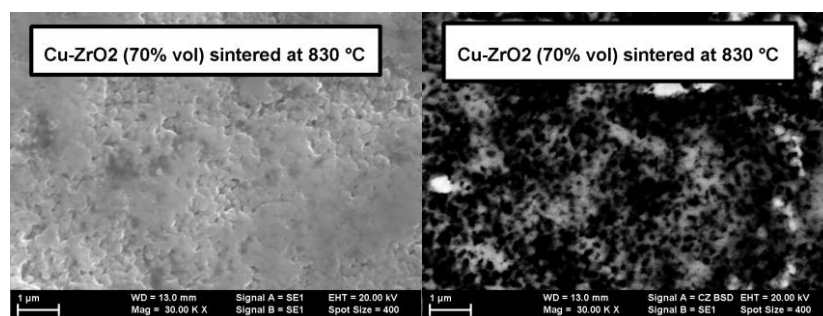
Morphological investigation of the samples is able to provide an answer for the unexpected good sintering behaviour. In figure 1 the densities of the produced samples are displayed as a function of the ZrO<sub>2</sub> volume content. The relative densities were calculated using the measured values in relation with the theoretical densities calculated using the direct mixing rule. The low temperature sintering curve exhibits an unusual trend, slightly increasing at lower concentrations (up to about 40% ZrO<sub>2</sub> volume, followed by a decrease toward a minimum and thereafter an increase to values close to 98%. Going to the maximum concentration results in a small amount of Cu lost from the sample and therefore also a decrease in density (because the Cu lost during SPS was not included in the theoretical density calculation). Higher temperature sintering is able to provide higher densities up to about 60% ZrO<sub>2</sub> volume concentration, then

the relative density starts to decrease and at 80% we have already melted Cu lost from the sample. For low temperature sintering, the increase of relative density at lower concentrations can be ascribed to better sintering. The SEM images presented in Figure 2 a and b show that ZrO<sub>2</sub> powders are agglomerated between the larger Cu grains. Increasing the ZrO<sub>2</sub> content and thus decreasing the Cu amount in the SPS implies an increase of the local temperature of Cu and as a result a better sintering and densities. However going to higher ZrO<sub>2</sub> content (above ~50% volume) brakes the contiguity of Cu in many areas and this leaves large ZrO<sub>2</sub> clusters with a subsequent lower quality sintering of the samples and lower relative densities (see Figure 2 c for the sample with 60% ZrO<sub>2</sub> sintered at 830 °C). On the other hand, sintering at higher temperatures (see Figure 2 d for the sample with 60% ZrO<sub>2</sub> sintered at 930 °C) brings Cu close to an almost fluid state and results in its infiltration through the ZrO<sub>2</sub> clusters, creating an uniform dispersion of small ZrO<sub>2</sub> clusters coated and joined by Cu metal.



**Fig. 2.** Cu- ZrO<sub>2</sub> composites' morphology for lower concentrations: a) EBS image of the 20% ZrO<sub>2</sub> sample sintered at 830 °C; b) SEM image of the 40% ZrO<sub>2</sub> sample sintered at 830 °C; c) SEM image of the 60% ZrO<sub>2</sub> sample sintered at 830 °C; d) EBS image of the 60% ZrO<sub>2</sub> sample sintered at 930 °C; Note that in EBS images the light greys correspond to high Z elements concentrations, while darker greys correspond to lower Z elements concentrations.

The same phenomena takes place also for increased ZrO<sub>2</sub> content in samples sintered at lower temperature. Figure 3 a and b illustrates this for the sample with 70% ZrO<sub>2</sub> volume concentration. The secondary emission image (Figure 3 a) shows the joined Cu coated ZrO<sub>2</sub> clusters while the backscattering image (Figure 3 b) proves the Cu infiltration (compare also with Figure 2 d for lower concentration higher temperature sintered probe).



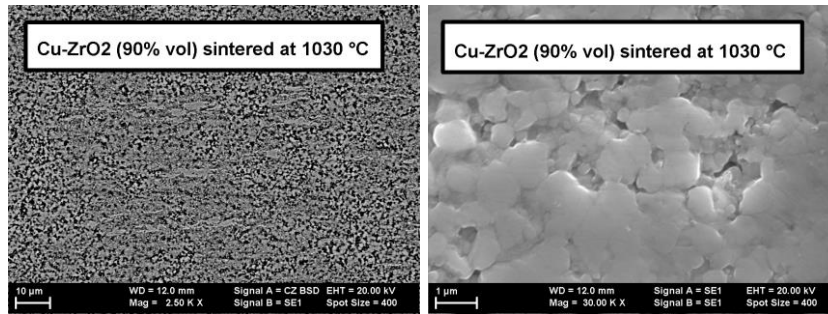


**Fig. 3.** Cu- ZrO<sub>2</sub> composites' morphology for higher concentrations: a) SEM image of the 70% ZrO<sub>2</sub> sample sintered at 830 °C; b) EBS image of the 70% ZrO<sub>2</sub> sample sintered at 830 °C; c) EBS image of the 90% ZrO<sub>2</sub> sample sintered at 1030 °C; d) SEM image of the 90% ZrO<sub>2</sub> sample sintered at 1030 °C; Note that in EBS images the light greys correspond to high Z elements concentrations, while darker greys correspond to lower Z elements concentrations.

Further increasing the ZrO<sub>2</sub> content and sintering temperature up to 90% ZrO<sub>2</sub> volume concentration and 1030 °C, respectively, is again able to provide a very fine structure of ZrO<sub>2</sub> small clusters coated with Cu (see Figure 3 c and d) but also results in a larger amount of Cu lost from the specimen. As the process is not really controlled it creates also larger pores in the sample, and therefore we'll not focus in this work further on such samples, which became also difficult to join to W and CuCrZr. As it can be deduced from Figure 1, an optimal sintering process can be obtained for ZrO<sub>2</sub> volume concentrations between 70% and 80% and average sintering temperatures close to 830 °C.

### 3.2. Thermophysical properties of the Cu-ZrO<sub>2</sub> specimens

To act as a thermal barrier a material should have lower thermal transport coefficients as the materials interfaced by it. This will allow the heat sink to work at a lower temperature. On the other side a strong insulating material might slow down too much the heat flow and thus producing the W armour overheating and its own as well. A good measure of the heat flow dynamic is provided by the thermal diffusivity which is a direct measure of the thermal inertia of materials. As we have done already with other materials [15], in figure 4 we analyse the experimental thermal diffusivity results obtained for the low temperature sintered Cu-ZrO<sub>2</sub> composites at the supposed temperature operating limits for the W-CuCrZr interface, namely 300 °C and 800 °C. It can be easily seen that already at 20% volume concentration of ZrO<sub>2</sub> the material can act as a thermal barrier. Moreover, for higher concentrations the diffusivity is lower as that of a Cu foam (63% porosity) commercial available material.

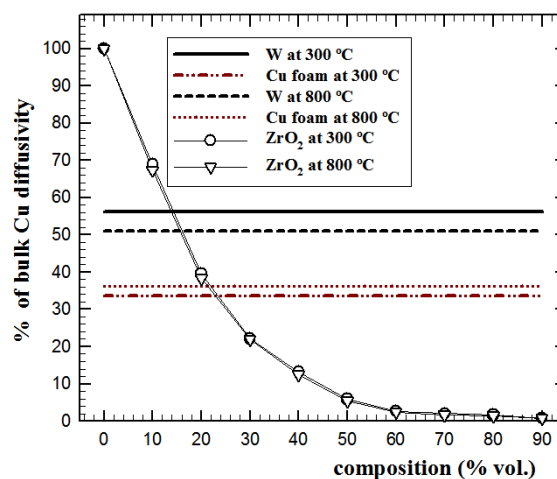


**Fig. 4.** Reduction of thermal diffusivity for Cu-ZrO<sub>2</sub> composites expressed as percent from pure Cu diffusivity at expected temperature operating window's limits.

For the DEMO W monoblock divertor concept very low thermal conductivity values are needed. In figure 5 we have plotted the thermal conductivity of some relevant Cu-ZrO<sub>2</sub> composites sintered at low temperature. One can easily see that for concentrations higher than about 55% volume the thermal conductivity values are below 10 W/m/K in all the temperature range from RT to 1000 °C. In this respect, the present materials outperform all the previous produced composites [15].

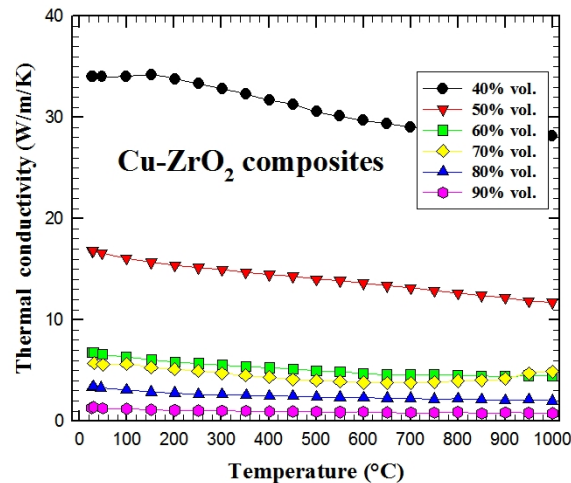


**Fig. 5.** Thermal conductivity of some typical low temperature sintered Cu – ZrO<sub>2</sub> thermal barrier composites.

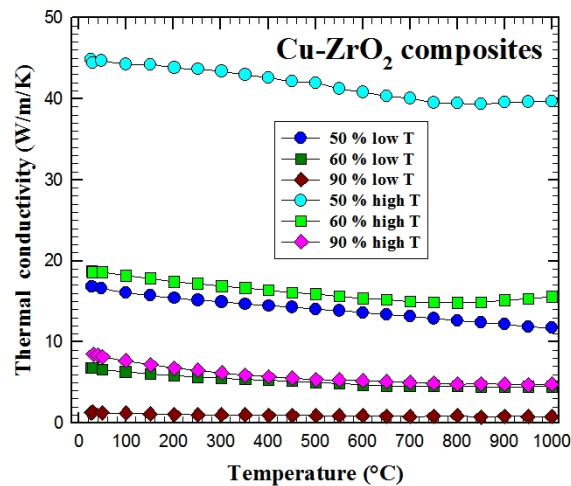


**Fig. 6.** Comparison of thermal conductivity values for Cu – ZrO<sub>2</sub> specimens sintered at lower (830 °C) and higher (930 °C) temperatures.

Since the samples' density depends on the processing temperature for intermediate concentrations we have also compared in figure 6 the thermal conductivity values for same compositions sintered at low and high temperature. For the samples with 50% and 60% ZrO<sub>2</sub> volume concentration the differences are significant, comparable with about 10% decrease of the ZrO<sub>2</sub> content for the sample with 60% sintered at higher temperature and even more for the sample with 50% content. However the difference is strongly reduced for the sample with 70 % oxide content and almost none for the sample with 80% content (not shown in Figure 6). For the sample with 90% volume ZrO<sub>2</sub> content the difference increase again but in this range uncontrolled melting of Cu and potential inhomogeneity creation in the sample might play an



important role.

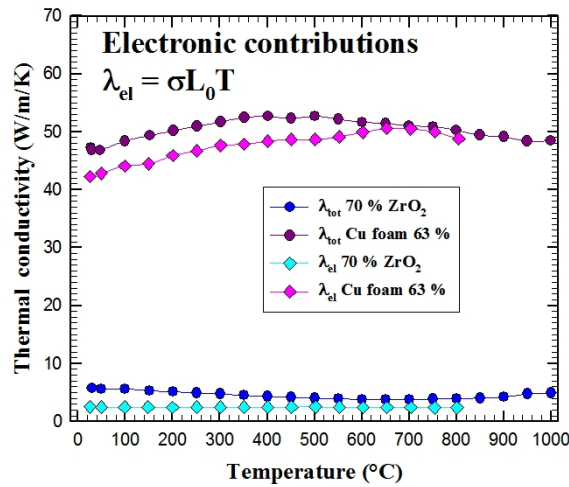


**Fig. 7.** Comparison of the total thermal conductivities and the electronic contributions to thermal conductivity for Cu – ZrO<sub>2</sub> specimen (70% volume) and Cu foam (63% porosity).

To better understand the thermal conduction mechanism in the samples we have also measured the electrical conductivity and for the 70% volume ZrO<sub>2</sub> sample and compared the result with the available Cu foam sample with 63 % porosity. Since the electrical conductivity is restrained to the metallic part of the composites, a qualitative estimation of the main mechanisms for the heat transfer can be performed using the Wiedeman-Franz law. In general the thermal conductivity is given by the sum of the electrons and phonons contributions. In the case of the Cu-ZrO<sub>2</sub> composites the electrons are moving only through the Cu part, similar to the case of Cu foam, while phonons contributions arise both from metal and oxide components. The electrons contribution to thermal conductivity, accordingly to Wiedeman-Franz law, is given by  $\lambda_{el} = \sigma L_0 T$ , where  $\sigma$  is the electrical conductivity,  $L_0$  the Lorenz number and  $T$  the temperature in K, with the Sommerfeld value for the Lorenz number,  $L_0 = 2.44 \times 10^{-8} \text{ W}\Omega\text{K}^{-2}$ . This later value can be considered adequate for simple metals like Cu but in other cases (e.g. intermetallic compounds or alloys) low temperature measurements are needed for both electrical and thermal conductivity in order to obtain an adequate value.

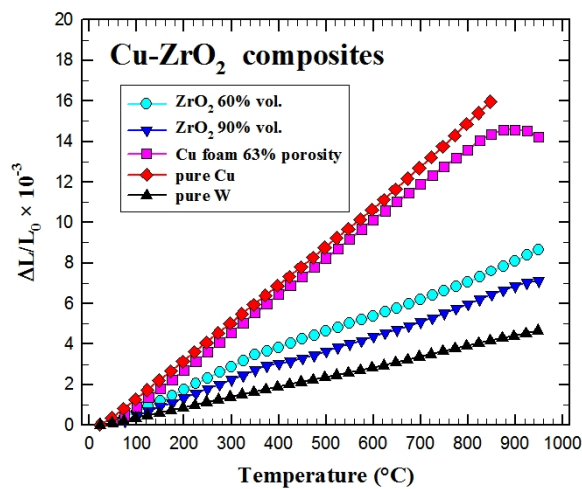


**Fig. 8.** Thermal expansion of some relevant Cu-ZrO<sub>2</sub> thermal barrier composites.

Based on these simple considerations, in figure 7 we have plotted the total thermal conductivity and the electronic contribution for the composite and Cu foam, respectively. While

in the case of Cu foam, the electrons' contribution accounts for over 90% of thermal conductivity, in the case of the Cu-ZrO<sub>2</sub> composite the electron contribution is limited to less than 50%. This can be explained by a non contiguity of the Cu net in the composite structure. Meanwhile, the phonons are transferring the heat also through oxide parts, albeit the strong scattering at the multiple interfaces of the nanometric ZrO<sub>2</sub> agglomerations. One should note that even the phonon contribution is reduced in the composite material to about half of the value obtained for the Cu foam.

Since the thermal barrier materials should be joined both to W armour and the CuCrZr heat sink it is desirable to have as thermal barrier a material able to mitigate the effects of the CTE mismatch in W and CuCrZr. The dilatometry measurement results plotted in figure 8 show that all materials with the suited thermal conductivity values fulfil this criterion, as opposed with the Cu foam which has a CTE close to that of pure Cu.

### 3.3. Implementation of thermal barriers in a 3-layers system.

One of the biggest advantages in having Cu in the thermal barrier composites is given by the fact that Cu can be easily joined to both W and other Cu alloys by various methods, diffusion bonding, brazing, FAST (field assisted sintering technique) joining or HRP (hot radial pressing, already used for ITER and DEMO divertor components). In the present work we have tested the FAST joining method which allows for short processing times. For low concentration ZrO<sub>2</sub> thermal barriers a one step process can be applied, meaning to join together all 3 materials in a single run. However, for high concentration ZrO<sub>2</sub> thermal barriers, in order to avoid the melting of either CuCrZr or/and Cu-ZrO<sub>2</sub> material a two steps process is needed. In the first run W is joined to the thermal barrier at a temperature of about 900 °C (in this case measured temperature) and then in the second run the obtained component is further joined to CuCrZr at a low temperature (700-800 °C, depending on the thermal barrier composition).

In order to estimate the joints quality we have used a thermal diffusivity measurement in a 2 layer configuration. The method was applied both to W-thermal barrier and CuCrZr-thermal barrier components produced by FAST. The results (shown in Figure S1 from the supplementary file) indicates a very low contact thermal resistance for the thermal barrier – CuCrZr interface (less than 10<sup>-7</sup> m<sup>2</sup>K/W) which was expected since both materials are Cu based. On the other hand the contact thermal resistance for W-thermal barrier interface is much higher, around 2 10<sup>-3</sup> m<sup>2</sup>K/W, which indicates a weak bonding. The value can be further decreased if the joining time is increased from 2 to 5 minutes. Also one should keep in mind that the second joining step will have a similar effect. A further test was performed on the final component (see e.g. figure S2 from the supplementary file) by measuring the thermal diffusivity of the interface material in a 3 layer model. In this case the value obtained includes also both contact thermal resistances and therefore is much lower as the value obtained for the same bare thermal barrier material (see figure S3 from the supplementary file). This result must be considered with caution, since the real dilatations of the materials can not be properly taken into account in the model.

## 4. Conclusions

Cu-ZrO<sub>2</sub> composites can be produced with high content oxide, up to 90% volume. For ZrO<sub>2</sub> composites with oxide content around 80% the highest densities are obtained, while the thermal conductivity values are below 10 W/m/K in the entire temperature range. An electric metallic conduction is preserved even for high oxide content materials. In the same time the thermal expansion coefficient has values around 7-8×10<sup>-6</sup> K<sup>-1</sup>, in-between W and Cu values. This properties make the present composites ideal for use as thermal barrier materials in the DEMO

divertor W-monoblock design. We have also demonstrated that these materials can be joined by FAST to both W and CuCrZr components. Further work will be devoted to optimize all the processing steps and to create pipe shaped materials.

## Acknowledgments

This work has been carried out within the framework of the EUROfusion Consortium and has received funding from the Euratom research and training programme 2014-2018 under grand agreement No 633053, WP-MAT and WP-EDU. The views and opinions expressed herein do not necessarily reflect those of European Commission.

## References

- [1] Sehila M. De Vicente G., Dudarev S., Rieth M., *Fus. Sci. and Techn.* **66** (2014) 38-45.
- [2] J.-Ha You, *Nucl. Fusion* **55** (2015) 113026.
- [3] T Hirai et al. *Physica Scripta* **T159** (2014) 014006.
- [4] N. Baluc et al., *Nucl. Fusion* **47** (2007) S696–S717.
- [5] K. Sugiyama et al., *Nucl. Fusion* **50** (2010) 035001.
- [6] M. W. Thompson, *Philosophical Magazine* **51**, (1960) 278-296.
- [7] L. Bukonte et al., *J. Appl. Phys.* **115** (2014) 123504
- [8] F. Ferroni et al, *Acta Materialia* **90** (2015) 380-393.
- [9] S.L. Wen et al., *Fus. Eng. Des.* **109** (2016) 569-573.
- [10] V. Barasbash et.al., *J. Nucl. Mater.* **367-370** (2007) 21-32.
- [11] D. Stork et al., *J. Nucl. Mater.* **455** (2014) 277-291.
- [12] J.H. You et al, *Fus. Eng. Des.* 109–111 (2016) 1598–1603
- [13] D. Maisonnier et al., *Nucl. Fusion* **47** (2007) 1524-1532.
- [14] T.R. Barrett et al., *Fus. Eng. Des.* **98–99** (2015) 1216-1220.
- [15] M. Galatanu et al, *Fus. Eng. Des.* (2017), <http://dx.doi.org/10.1016/j.fuseng-des.2017.02.031>
- [16] A. Li-Puma et al., *Fus. Eng. Des.* **88** (2013) 1836-1843.
- [17] W. Shen et al., *Fusion Sci. Technol.*, **66** (2014) 260-265.
- [18] G. Pintsuk, et al., *Fus. Eng. Des.*, **66–68** (2003) 237-240.
- [19] Z. Zhou et al., *J. Nucl. Mater.* **363–365** (2007) 1309-1314.
- [20] J. H. You et al., *J. Nucl. Mater.* **438** (2013) 1–6.
- [21] M. Schöbel et al., *J. Nucl. Mater.* **409** (2011), 225-234.
- [22] S. Grasso et al, *Sci. Technol. Adv. Mater.* **10** (2009) 053001
- [23] M. Suárez et al. *Materials Science: “Sintering Applications”* (2013) ed. Burcu Ertuğ, ISBN 978-953-51-0974-7.